



# A NEW SOLUTION FOR TACKLING MISMATCHING LOSSES IN SOLAR PV ARRAY VIA IMAGE ENCRYPTION

Karthick B.<sup>1</sup>, Vengatesan V.<sup>2</sup>, Amala Arockia Raj J.<sup>3</sup>, Kumara Swamy I.<sup>4</sup> and Venkateswaran Madhu<sup>5</sup>

<sup>1</sup>Department of Electrical and Electronics Engineering, Madanapalle Institute of Technology and Sciences, Madanapalle, Andhra Pradesh, India

<sup>2</sup>Department of Electrical and Electronics Engineering, SRM TRP Engineering College, Tiruchirappalli, Tamil Nadu, India

<sup>3</sup>Department of Electrical and Electronics Engineering, J. J. College of Engineering and Technology, Tiruchirappalli, Tamil Nadu, India

<sup>4</sup>Department of Electrical and Electronics Engineering, Sree Vidyanikethan Engineering College/MB University, Tirupati, Andhra Pradesh, India

<sup>5</sup>Department of Electrical and Electronics Engineering, Lendi Institute of Engineering and Technology, Vizianagaram, Andhra Pradesh, India

E-Mail: [bkarthick39@gmail.com](mailto:bkarthick39@gmail.com)

## ABSTRACT

Solar photovoltaic systems may undergo changes in power generation due to environmental factors such as partial shading, resulting in losses due to mismatch. This can ultimately lead to a decrease in the efficiency of the system's power conversion. While current solutions are both cost-effective and efficient, there is potential for novel approaches to further enhance system performance by improving consistency, power production, and minimizing mismatch losses. To address these limitations, this paper proposes the utilization of a highly efficient generalized Arnold's cat Map technique, commonly used in the image encryption process, to reconfigure the PV array. The effectiveness of these proposed approaches is evaluated in a MATLAB Simulink environment, specifically for a symmetrical (8x8) PV array, under various benchmark conditions such as Long wide; Short wide, Long Narrow, and Short Narrow shading conditions. The results obtained from these evaluations are then compared to prominent strategies such as Total-cross-tied and the recently reported Chaotic Baker's Map reconfiguration techniques. Furthermore, extensive analysis is conducted using different performance indices to gain a comprehensive understanding of the proposed approaches.

**Keywords:** Arnold's cat map, global maximum power point, partial shading, mismatch loss, fill-factor.

Manuscript Received 13 April 2024; Revised 20 July 2024; Published 5 September 2024

## INTRODUCTION

The challenges related to shading encountered by photovoltaic (PV) panels are inevitable and arise from a multitude of factors including towering structures, the accumulation of dust particles, bird excrement, transient clouds, vegetation, poles, and the presence of overhead transmission lines (Ahmad, R *et al.*, 2017). These shading issues can create hotspots in the PV module array, which can be a fire hazard and cause damage to the panel. To ensure the longevity of PV panels, it is important to detect hotspots and faults early on using appropriate methods such as visual examination, infrared thermography, and ultraviolet fluorescence imaging (P. Guerriero *et al.*, 2019). During periods of low irradiation, the installation of bypass diodes serves as a preventive measure against hotspots by redirecting the current. However, this approach may lead to the emergence of multiple peaks in the array characteristics, consequently diminishing the overall output (Rahman, M *et al.*, 2021). As a result, many MPPT techniques can get stuck in a local peak, leading to power loss. To surpass this constraint and optimize the output beyond the level attained solely with MPPT, reconfiguration methods are employed (Celikel, R *et al.*, 2022).

There are two primary methods for reconfiguring shaded modules: Dynamic and Static PV reconfiguration. Dynamic photovoltaic reconfiguration involves modifying the electrical connections of photovoltaic modules (PV

modules) by utilizing a continuous switching matrix. The objective of this method is to increase the power output when the modules are exposed to shading conditions (Karakose, M *et al.*, 2022). Numerous research studies have been conducted in the field of dynamic reconfigurability for photovoltaics. In the study conducted by Deshkar *et al.* (2015), a highly effective strategy for reconfiguration is introduced, which utilizes shadow detection and optimization techniques based on image processing. This approach utilizes image processing to gather shadow information, and optimization is performed using a clonal selection method. Nevertheless, the implementation of this strategy necessitates the utilization of switching matrices, intricate algorithms, a monitoring camera for shading assessment, and additional supplementary components. To mitigate fluctuations in row current and minimize the occurrence of multiple local maximum power peaks (MPPs) in the array's characteristics, numerous population-based metaheuristic algorithms have been proposed. These include the genetic algorithm (GA) as presented by Babu *et al.* (2018), particle swarm optimization (PSO) as explored by Yousri *et al.* (2021), and the modified harries hawk (MHH) algorithm as introduced by Anjum *et al.* (2022).

The use of dynamic reconfiguration techniques improves the output by reducing mismatch losses caused by shading. However, this method necessitates the use of numerous intricate switches, complex algorithms to



control these switches, sophisticated control units, efficient driver circuits, sensors, systematic monitoring units, and composite wiring. As a result, the overall system becomes overly complex and economically inefficient.

Static photovoltaic (PV) reconfiguration technologies employ a fixed interconnect system to enhance power generation in the presence of partial shading. This is accomplished by minimizing fluctuations in row current without requiring electrical connections or a switching matrix. Extensive research has been carried out on static PV array reconfigurations, and studies have shown the efficacy of classical sudoku and optimal sudoku methods in boosting power output under PSC, as evidenced by references (S. Mikkili *et al.*, 2022) and (C.-E. Ye *et al.*, 2021). These methods preserve the pre-existing electrical connections between modules.

The distribution of shading effects across a shaded PV array was attempted by providing a free sudoku problem (R. K. Pachauri *et al.*, 2022). To increase power output, the impact of shadows on the PV array was dispersed using Magic Square puzzle architecture (M. S. S. Nihanth *et al.*, 2019). In (D. S. Pillai *et al.*, 2021) and (B. Dhanalakshmi *et al.*, 2018), the Skyscraper and Chess-Knight puzzles were created respectively to minimize shading impact and maximize power output. To reduce voltage and power loss, certain literature such as the Dominance Square (B. Dhanalakshmi *et al.*, 2020), Competence Square (S. S. Reddy *et al.*, 2020), and Odd-Even Prime (OEP) (S. S. Reddy *et al.*, 2021) utilize rearrangement of rows and columns when extending wire length. The Lo-shu technique (R. Venkateswari *et al.*, 2020) proposes physically relocating photovoltaic modules without altering electrical connections to mitigate the impact of partial shading on a (9 × 9) photovoltaic array. A mathematical relation-based Calcudoku puzzle (B. Aljafari *et al.*, 2023) has recently been suggested to improve power consistency and reduce mismatching losses in the PV array. However, despite their compatibility, these techniques have inadequate shading distribution, resulting in increased mismatch losses. The potential of reconfiguring the PV array using image encryption-based chaotic mapping techniques has not been thoroughly investigated by the researchers.

In this study, a novel approach known as Image encryption utilizing Arnold's cat mapping technique has been proposed to enhance the efficiency of photovoltaic (PV) arrays. This approach is suitable for arrays of various sizes, including (5×5), (7×9), (23×17), and more. To analyze its effectiveness, a symmetrical PV array of size (8×8) is investigated and contrasted with conventional reconfiguration methods like Total-cross-tied (TCT) and Chaotic-baker's Map (CBM) under different shading conditions.

Moreover, it will be effective for solving some risky PQ challenges caused by the nature of the load which is associated with the source and grid to sustain the voltage undistorted. The manuscript is structured to this extent. Section II gives the Equivalent circuit of the PV module. Section III gives the proposed methodology of the

paper. Section IV focuses on Two-dimensional Arnold's cat mapping method. Section V gives different parametric metrics of the PV module. Section VI gives the Simulation results and discussions for various benchmark shading conditions. At last, the conclusion of the paper finds a place in Section VII.

## PV MODULE EQUIVALENT CIRCUIT

The PV array's performance evaluation greatly relies on the modeling of the PV cell, which is a crucial factor. There are different approaches to modeling PV cells, such as the one-diode, two-diode, and three-diode models (F. E. Ndi *et al.*, 2021), which can be found in the literature. These models, however, necessitate resilient algorithms for extracting the unidentified parameters and attaining enhanced accuracy. In particular, the three-diode model has not been extensively studied due to the complexity of its calculations. Additionally, including an extra diode increases the complexity, processing time, and computational burden involved in determining the unknown parameters. Therefore, this study utilizes a single diode model (see Figure-1), which still provides acceptable accuracy.

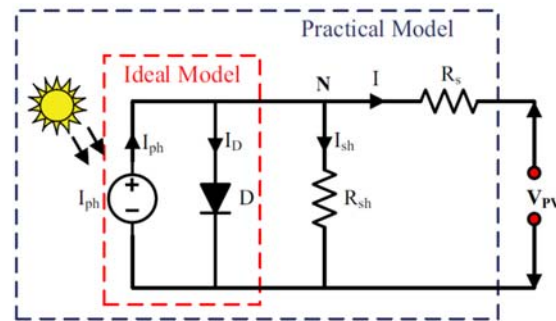


Figure-1. A one-diode equivalent circuit model.

The essential condition that portrays the I-V attributes of the PV model is determined by

$$I = I_L - I_0 \left( e^{\frac{q(V+IR_s)}{kT}} - 1 \right) - \left( \frac{V+IR_s}{R_{sh}} \right) \quad (1)$$

where,

I is the current (A),  $I_L$  is the light generated current (A),  $I_0$  is the diode saturation current (A),  $q$  is the charge of an electron ( $1.6 \times 10^{-19}$ ) coulomb,  $K$  is the Boltzmann constant (j/K),  $T$  is the Temperature (K),  $R_{sh}$  and  $R_s$  are the series and shunt resistance ( $\Omega$ ) and  $V$  is the Output voltage (V).

## PROPOSED METHODOLOGY

Typically, a digital image is structured as a 2D ( $m \times n$ ) matrix, where the dimensions "m" and "n" correspond to the rows and columns of the matrix, respectively. To ensure the security of the image, the process of encrypting it involves the random substitution



of the original pixel positions with a specific transformation, as stated by X. Kang et al. in 2019. However, through the repeated application of this transformation, the original image can be reconstructed. This reconstruction is made possible by modifying the pixel positions using a private-key algorithm that can only be deciphered by authorized end-users. Among the commonly employed techniques for image encryption, 2D chaotic map algorithms, as described by T. Li et al. in 2020, are widely utilized. These algorithms typically represent the two-dimensional maps in a specific format.

$$\begin{cases} x_{i+1} = r(x_i, y_i) \\ y_{i+1} = s(x_i, y_i) \end{cases} \quad (2)$$

The application of the chaotic map algorithm involves the utilization of the functions "r" and "s" to reposition the original pixel coordinates  $(x_i, y_i)$  of a digital image. This repositioning process results in the generation of new pixel coordinates  $(x_{i+1}, y_{i+1})$ , thereby creating an encrypted image that offers improved security. The image encryption procedure, along with the generalized pseudo code of the ACM techniques for rearranging the elements of the matrix, can be observed in Figure-2. In a  $(3 \times 3)$  matrix, the numbers 1 to 9 are arranged in a row-wise manner. Through the implementation of a chaotic map, these numbers undergo scrambling, as depicted in Figure-2 (b). By utilizing the rearranged matrix obtained through the chaotic map approach, the pixel coordinates of the original matrix transform into new pixel coordinates.

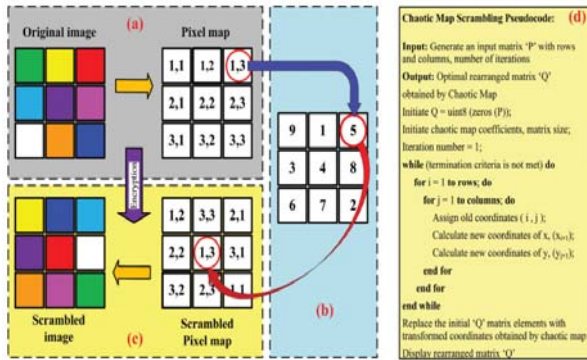


**Figure-2.** Image encryption process (a) Original image (b) rearranged matrix (c) scrambled image (d) Generalized pseudocode of the proposed ACM techniques.

**TWO-DIMENSIONAL ARNOLD'S CAT MAP**

The Arnold's Cat Map (ACM) is a chaotic system that was developed by Vladimir I. Arnold, a mathematician from Russia, in 1960. The name "Arnold's cat map" came about from an experiment that involved an image of a cat (Li, C *et al.*, 2022).

The equation representing Arnold's Cat Map is described as follows:

$$\begin{pmatrix} x_{i+1} \\ y_{i+1} \end{pmatrix} = \begin{pmatrix} 1 & 1 \\ 1 & 2 \end{pmatrix} * \begin{pmatrix} x_i \\ y_i \end{pmatrix} \text{ mod } 1 \quad (3)$$

$$\begin{pmatrix} x_{i+1} \\ y_{i+1} \end{pmatrix} = \begin{pmatrix} 1 & a \\ b & ab+1 \end{pmatrix} * \begin{pmatrix} x_i \\ y_i \end{pmatrix} \text{ mod } N \quad (4)$$

The ACM algorithm is used to transform the old pixel locations  $(x_i, y_i)$  to the new pixel locations  $(x_{i+1}, y_{i+1})$  in Figure-3. Eq. (4) involves the system control parameters 'a' and 'b', while 'N' represents the size of the encrypted image. The old pixel locations  $(x_i, y_i)$  and the new pixel locations  $(x_{i+1}, y_{i+1})$  are denoted by  $x_i$  and  $y_i$ , and  $x_{i+1}$  and  $y_{i+1}$  respectively.

11	12	13	14	15	16	17	18
21	22	23	24	25	26	27	28
31	32	33	34	35	36	37	38
41	42	43	44	45	46	47	48
51	52	53	54	55	56	57	58
61	62	63	64	65	66	67	68
71	72	73	74	75	76	77	78
81	82	83	84	85	86	87	88

(a)

88	51	22	73	44	15	66	37
76	47	18	61	32	83	54	25
64	35	86	57	28	71	42	13
52	23	74	45	16	67	38	81
48	11	62	33	84	55	26	77
36	87	58	21	72	43	14	65
24	75	46	17	68	31	82	53
12	63	34	85	56	27	78	41

(b)

**Figure-3.** Original matrix and reconfigured matrix obtained by proposed ACM technique.

**PERFORMANCE PARAMETERS**

The effectiveness of the suggested methods is assessed based on the following criteria:

**Global Maximum Power Point (GMPP)**

The PV array's maximum power output represents the highest amount of power that can be harnessed from it.

**Mismatching Power Loss**

It is fundamental to broaden any model comparable to its idealistic features. The modeling of Solar PV (Photovoltaic System) and its design calculations for D-STATCOM is described elaborately.

$$MM_p (W) = GMP_{STC} - GMP_{PSC} \quad (5)$$

**Fill-Factor (FF)**

The efficiency of solar panels can be determined by the fill factor, which is a vital parameter. The fill factor is obtained by dividing the actual rated maximum power ( $P_{max}$ ) by the theoretical maximum power ( $I_{sc} \times V_{oc}$ ). Solar panels with higher fill factors encounter fewer losses caused by resistances in the cells, whether they are in series or parallel.

$$\text{Fill-Factor} = \frac{V_{mpp} \times I_{mpp}}{V_{oc} \times I_{oc}} = \frac{P_{max}}{V_{oc} \times I_{oc}} \quad (6)$$



**Power Losses**

The term refers to the ratio between the difference in the global maximum power point (GMPP) of a photovoltaic (PV) array under standard test conditions (STC) and the GMPP under partially shaded conditions (PSC), divided by the GMPP at STC.

$$\text{Power-loss} = \left[ \frac{GMPP_{STC} - GMPP_{PSC}}{GMPP_{STC}} \right] \quad (7)$$

**SIMULATION RESULTS AND DISCUSSIONS**

The analysis and testing of the conventional TCT, existing CBM, and proposed ACM re-configurations have been conducted for a 335W, (8 × 8) PV array in MATLAB. The PV array has a nominal voltage and current at Pmax of 38.1 V and 8.80 A, respectively. Various benchmark shading scenarios, such as Long wide, short wide, Long Narrow, and Short Narrow patterns, were used in the experiments. The performance of the system was evaluated using performance indices like Fill factor, Power loss, and Mismatch loss, with the help of a Vikram Solar Eldora 335W PV Panel. The simulations were performed on a MATLAB/SIMULINK Platform, which was equipped with a Dual-Core Processor, 2.2GHz memory size, and 8GB RAM.

**Analysis of Long-Wide (LW) Shading Pattern**

The main objective of testing any method for re-configuring a PV array is to guarantee the efficient dispersion of shade, especially in situations with intense shade levels. To achieve this objective, the Long Wide (LW) shade pattern is employed. This particular shade scenario is noteworthy due to the substantial shading that occurs on the panels. Consequently, a significant portion of the PV array’s column and row is impacted by shade, specifically the last three columns and rows. These specific areas are exposed to five distinct levels of irradiance: 1000 W/m<sup>2</sup>, 600 W/m<sup>2</sup>, 500 W/m<sup>2</sup>, 400 W/m<sup>2</sup> and 200 W/m<sup>2</sup> as shown in Figure-4.

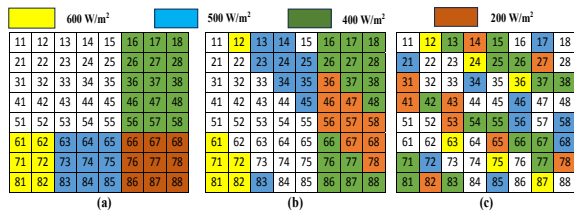


**Figure-4.** LW shading case: (a) TCT, (b) CBM, (c) Proposed ACM.

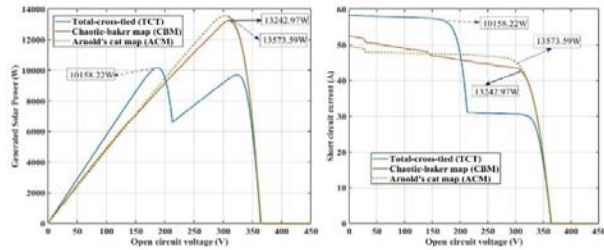


**Figure-5.** P-V and I-V characteristics under LW shading pattern.

From the P-V characteristics shown in Figure-5, it is evident that the proposed ACM configurations exhibit a considerably reduced number of maximum power points (MPPs) in comparison to alternative configurations. As a result, the PV array characteristics are smoother. Additionally, the proposed ACM configurations lead to a reduction in both mismatch power and power loss, with values of 7741.39 W and 36.31 W respectively. Furthermore, the fill factor is significantly higher at 31.21. The enhanced values of performance indices in Table 1 validate the superior performance of the suggested configurations compared to TCT and CBM.

**Analysis of Short-Wide (SW) Shading Pattern**

It is a common occurrence to come across a Short Wide (SW) shade in photovoltaic arrays, which is caused by the shadows cast by poles. This shade leads to only half of the panel being completely shaded, while the other half remains exposed to the full intensity of irradiance. To study and analyze this phenomenon, a (8 × 8) PV array was used and subjected to three different levels of insolation. The last three rows of the array had shading in three columns, with varying irradiances of 600 W/m<sup>2</sup>, 400 W/m<sup>2</sup>, and 200 W/m<sup>2</sup>. On the other hand, the initial five columns of the sixth row received 600 W/m<sup>2</sup> shadings, while the remaining panels were exposed to full irradiance at 1000 W/m<sup>2</sup>, as shown in Fig.6 respectively.

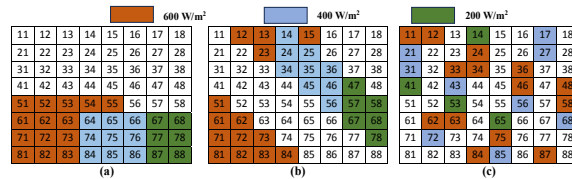


**Figure-6.** SW shading case: (a) TCT, (b) CBM, (c) Proposed ACM.

From the P-V characteristics shown in Figure-7, it is evident that the proposed ACM configurations exhibit a considerably reduced number of maximum power points (MPPs) in comparison to alternative configurations. As a result, the PV array characteristics are smoother. The ACM re-configuration methods proposed also demonstrate exceptional performance during PS conditions, achieving the lowest power mismatch power of 7741.39W and the



highest fill factor of 0.3647 under short wide (SW) shading conditions, as shown in Table-1. This sets them apart from both conventional and existing CBM configurations, emphasizing their superiority.

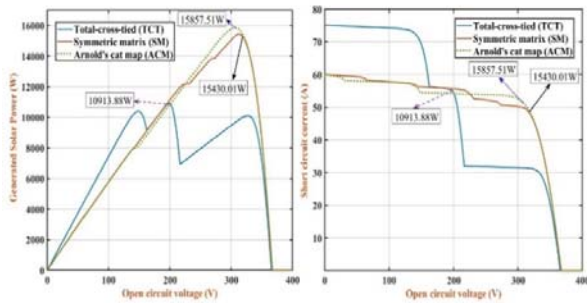


Figure-7. P-V and I-V characteristics under SW shading pattern.

**Analysis of Long-Narrow (LN) Shading Pattern**

The effectiveness of the PV array is not solely determined by the placement of shading; the intensity of the shading also plays a vital role. Even if there are fewer cells in a row, they can still be impacted when a significant portion of the array is shaded. The Long Narrow (LN) shading pattern utilizes four different irradiation profiles, specifically: 1000 W/m<sup>2</sup>, 700 W/m<sup>2</sup>, 400 W/m<sup>2</sup>, and 300 W/m<sup>2</sup>, as shown in Figure-8 in a scrambled order.

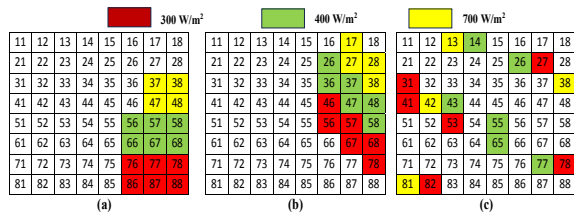


Figure-8. LN shading case: (a) TCT, (b) CBM, (c) Proposed ACM.

The proposed ACM method, which evenly distributes shade across the entire array, generates significantly more power compared to traditional re-configuration methods like TCT and CBM. According to the P-V characteristic curves in Figure-9, the optimal power achieved by TCT, CBM, and the proposed ACM are 16860.89 W, 17216.18 W, and 18000 W respectively. Table-1 shows that the mismatched power obtained by TCT, CBM, and the proposed ACM are 4454.09 W, 4098.80 W, and 3315.68 W respectively. By implementing the proposed ACM configurations, the corresponding power loss is significantly reduced to 15.55 W and the fill factor is increased to 0.4139.

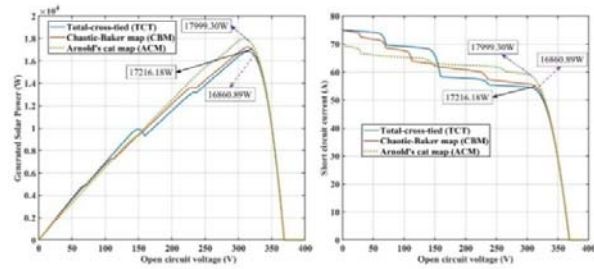


Figure-9. P-V and I-V characteristics under LN shading pattern.

**Analysis of Short-Narrow (SN) Shading Pattern**

The Short Narrow (SN) shading pattern is utilized in a specific area of an (8 × 8) photovoltaic (PV) array. This shaded portion is found in both the column and row, and it experiences a reduced level of irradiance, measuring 600 W/m<sup>2</sup> and 400 W/m<sup>2</sup> respectively. In contrast, the remaining part of the panel receives the maximum irradiance of 1000 W/m<sup>2</sup> as shown in Figure-10.

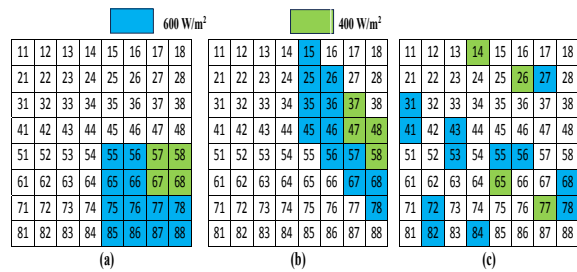


Figure-10. SN shading case: (a) TCT, (b) CBM, (c) Proposed ACM.

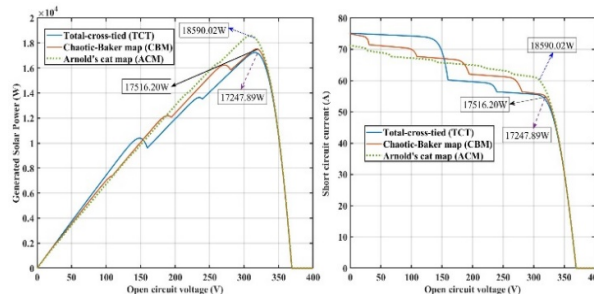


Figure-11. P-V and I-V characteristics under SN shading pattern.

The optimal powers for the TCT, CBM, and proposed ACM in Figure-10 are 17247.89 W, 17516.20 W, and 18590.02 W, respectively, as shown by the P-V curves. According to Table 1, the mismatch powers for TCT, CBM, and proposed ACM are 4067.09 W, 3798.78 W, and 2724.96 W, respectively. By implementing the proposed ACM configurations, the corresponding power loss is significantly reduced to 12.784 W, and a higher fill factor of 0.4275 is achieved.

**Table-1.** Estimation of performance indices for benchmark shading patterns.

Shading Pattern	Configuration	Mis-matching Loss (W)	Fill Factor	Power Loss
LW	TT	11,1576.76	23.36	52.342
	CBM	8,072.01	30.45	37.870
	Proposed ACM	7,741.39	31.21	36.319
SW	TCT	10,401.12	25.10	48.798
	CBM	5,884.97	35.48	27.609
	Proposed ACM	5,457.47	36.47	25.603
LN	TCT	4,454.09	38.78	20.896
	CBM	4,098.80	39.59	19.229
	Proposed ACM	3,315.68	41.39	15.555
SN	TCT	4,067.09	39.67	19.080
	CBM	3,798.78	40.28	17.821
	Proposed ACM	2,724.96	42.75	12.784

## CONCLUSIONS

This study presents a novel image encryption application that utilizes Arnold's cat map technique to distribute shadows through array reconfiguration, resulting in a highly efficient system. The proposed configuration, known as ACM, is extensively evaluated for an  $(8 \times 8)$  PV array size under various shading conditions. To assess its effectiveness, the performance of the ACM method is compared and analyzed against conventional interconnection schemes such as Total-cross-tied (TCT) and chaotic-baker map (CBM). Among these approaches, the ACM method achieves the highest fill factor of 31.21, 36.47, 41.39, and 42.75 for all shading conditions. Consequently, it can be concluded that the utilization of reconfiguration techniques based on Arnold's cat map is essential for enhancing output and minimizing mismatch losses during partial shading conditions, thereby ensuring superior and reliable performance.

## REFERENCES

- [1] Ahmad R., A. M. Sher, U. T. Shami, S. Olalekan and S. Olalekan. 2017. An analytical approach to study partial shading effects on PV array supported by literature. *Renew and Sustain Ener. Rev.* 74: 721-32.
- [2] P. Guerriero and S. Daliento. 2019. Toward a hot spot-free PV module. *IEEE J. Photovolt.* 9(3): 796-802.
- [3] Rahman M. M., I. Khan and K. Alameh. 2021. Potential measurement techniques for photovoltaic module failure diagnosis: A review. *Renewable and Sustainable Energy Reviews.* 151: 111532.
- [4] Celikel R., M. Yilmaz and A. Gundogdu. 2022. A voltage scanning-based MPPT method for PV power systems under complex partial shading conditions. *Renewable Energy.* 184: 361-73.
- [5] F. Belhachat, C. Larbes. 2021. PV array reconfiguration techniques for maximum power optimization under partial shading conditions: A review. *Solar Energy.* 230: 558-582.
- [6] Karakose M., M. Baygin, K. Murat, N. Baygin and E. Akin. Fuzzy-based reconfiguration method using intelligent partial shadow detection in PV arrays. *International Journal of Computational Intelligence Systems.* 9(2): 202-12.
- [7] Deshkar S. N., S. B. Dhale, J. S. Mukherjee, T. S. Babu and N. Rajasekar. 2015. Solar PV array reconfiguration under partial shading conditions for maximum power extraction using genetic algorithm. *Renewable and Sustainable Energy Reviews.* 43: 102-10.
- [8] Babu T. S., J. P. Ram, T. Dragičević, M. Miyatake, F. Blaabjerg and N. Rajasekar. 2018. Particle swarm optimization-based solar PV array reconfiguration of the maximum power extraction under partial shading conditions. *IEEE Transactions on Sustainable Energy.* 9(1): 74-85.
- [9] Yousri D., D. Allam, and M. B. Eteiba. 2021. Optimal photovoltaic array reconfiguration for alleviating the partial shading influence based on a modified Harris Hawks optimizer. *Energy Conversion and Management.* 206: 112470.



- [10] S. Anjum, V. Mukherjee, G. Mehta. 2022. Modelling and simulation of addoku based reconfiguration technique to harvest maximum power from the photovoltaic array under partial shading conditions. *Simulation Modelling Practice and Theory*. 115, 102447.
- [11] S. Mikkili, K. A. Bapurao, P. K. Bonthagorla. 2022. Sudoku and optimal sudoku reconfiguration techniques for power enhancement of partial shaded solar PV system. *Journal of the Institution of Engineers (India): Series B*. 103(5): 1793-1807.
- [12] C.-E. Ye, C.-C. Tai, Y.-P. Huang, J.-J. Chen. 2021. Dispersed partial shading effect and reduced power loss in a PV array using a complementary sudoku puzzle topology. *Energy conversion and management*. 246: 114675.
- [13] R. K. Pachauri, S. B. Thanikanti, J. Bai, V. K. Yadav, B. Aljafari, S. Ghosh, H. H. Alhelou. 2022. Ancient Chinese magic square-based PV array reconfiguration methodology to reduce power loss under partial shading conditions. *Energy Conversion and Management*. 253: 115148.
- [14] M. S. S. Nihanth, J. P. Ram, D. S. Pillai, A. M. Ghias, A. Garg, N. Rajasekar. 2019. Enhanced power production in PV arrays using a new skyscraper puzzle-based one-time reconfiguration procedure under partial shade conditions (PSCs). *Solar Energy*. 194: 209-224.
- [15] D. S. Pillai, J. P. Ram, V. Shabunko, Y.-J. Kim. 2021. A new shade dispersion technique is compatible with symmetrical and unsymmetrical photovoltaic (PV) arrays. *Energy* 225.
- [16] B. Dhanalakshmi, N. Rajasekar. 2018. Dominance square-based array reconfiguration scheme for power loss reduction in solar photovoltaic (PV) systems. *Energy conversion and management*. 156: 84-102.
- [17] B. Dhanalakshmi, N. Rajasekar. 2018. A novel competence square-based PV array reconfiguration technique for solar PV maximum power extraction. *Energy conversion and management*. 174: 897-912.
- [18] S. S. Reddy, C. Yammani. 2020. Odd-even-prime pattern for PV array to increase power output under partial shading conditions. *Energy*. 213: 118780.
- [19] R. Venkateswari, N. Rajasekar. 2020. Power enhancement of PV system via physical array reconfiguration based Lo-shu technique. *Energy Conversion and Management*. 215: 112885.
- [20] B. Aljafari, S. Devakirubakaran, C. Bharatiraja, P. K. Balachandran, T. S. Babu. 2023. Power-enhanced solar PV array configuration based on calcudoku puzzle pattern for partial shaded PV system. *Heliyon*. 9(5).
- [21] F. E. Ndi, S. N. Perabi, S. E. Ndjakomo, G. O. Abessolo, G. M. Mengata. 2021. Estimation of single-diode and two-diode solar cell parameters by equilibrium optimizer method. *Energy Reports*. 7: 4761-4768.
- [22] X. Kang and R. Tao. 2019. Color image encryption using pixel scrambling operator and reality-preserving MPFRHT. *IEEE Trans. Circuits Syst. Video Technol.* 29(7): 1919-32.
- [23] T. Li, B. Du and X. Liang. 2020. Image encryption algorithm based on logistic and two-dimensional Lorenz. *IEEE Access*. 8: 13792-805.
- [24] Li, C., K. Tan, B. Feng, and J. Lu. 2022. The graph structure of the generalized discrete Arnold's cat map. *IEEE Transactions on Computers*. 71(2): 364-77.